LETTERS

LRRC26 auxiliary protein allows BK channel activation at resting voltage without calcium

Jiusheng Yan[1] & Richard W. Aldrich[1]

Large-conductance, voltage- and calcium-activated potassium (BK, or $K_{Ca}1.1$) channels are ubiquitously expressed in electrically excitable and non-excitable cells[1,2], either as α-subunit (BKα) tetramers or together with tissue specific auxiliary β-subunits (β1–β4)[3–5]. Activation of BK channels typically requires coincident membrane depolarization and elevation in free cytosolic Ca^{2+} concentration ($[Ca^{2+}]_i$)[6,7], which are not physiological conditions for most non-excitable cells. Here we present evidence that in non-excitable LNCaP prostate cancer cells, BK channels can be activated at negative voltages without rises in $[Ca^{2+}]_i$ through their complex with an auxiliary protein, leucine-rich repeat (LRR)-containing protein 26 (LRRC26). LRRC26 modulates the gating of a BK channel by enhancing the allosteric coupling between voltage-sensor activation and the channel's closed–open transition. This finding reveals a novel auxiliary protein of a voltage-gated ion channel that gives an unprecedentedly large negative shift (∼−140 mV) in voltage dependence and provides a molecular basis for activation of BK channels at physiological voltages and calcium levels in non-excitable cells.

BK channels are critically involved in diverse physiological processes in both electrically excitable and non-excitable tissues. The BKα subunit (∼130 kDa) is encoded by a single gene, and diversity in the physiological properties of BK channels is generated by accessory β-subunits[3–5], alternative splicing of the precursor messenger RNA[8], or post-translational phosphorylation[9,10] and methionine oxidation[11]. In spite of the variability, the required voltage or $[Ca^{2+}]_i$ alone for BK channel activation is generally too high, with a half-activation voltage of $V_{1/2} > 100$ mV at $[Ca^{2+}]_i = 0$ or a half-maximal effective calcium concentration of $EC_{50} \geq 10\,\mu M$ at resting membrane potentials, to be within the physiological range under resting conditions (Supplementary Fig. 1a). Thus, in excitable cells it is generally found that BK channel opening involves simultaneous activation by both membrane depolarization and increased $[Ca^{2+}]_i$ (refs 6, 7). This raises questions about the function of BK channels in non-excitable cells, which have negative membrane voltages (≤−40 mV) and a relatively constant low value of $[Ca^{2+}]_i$ (≤100 nM). LNCaP prostate cancer cells possess an unusual BK-type K^+ channel that can be activated at resting voltages and $[Ca^{2+}]_i$ (ref. 12). We have investigated the molecular basis underlying the activation of this unconventional LNCaP BK channel.

As previously reported[12], LNCaP cells show a pronounced K^+ current in the nominal absence of $[Ca^{2+}]_i$ that is easily detectable at voltages above 0 mV in excised inside-out patches (Fig. 1a). The relationship between open probability (P_o) and voltage can be fitted with a single Boltzmann function with $V_{1/2} = 25 \pm 3$ mV. This K^+ channel had a large single-channel conductance (∼250 pS), was activated by $[Ca^{2+}]_i$ and fully blocked by the BK-channel-specific blocker paxilline (100 nM). These electrophysiological properties are characteristics of typical BK channels except for the capacity to activate at low voltages in the nominal absence of $[Ca^{2+}]_i$. We refer to this LNCaP K^+ channel as a low-$V_{1/2}$ BK channel. This is in contrast to the typical BK channels formed by BKα alone, which requires high voltages of more than 100 mV to open with a $V_{1/2}$ of ∼165 mV at $[Ca^{2+}]_i = 0$ (Fig. 1a). We refer to these typical BK channels as high-$V_{1/2}$ BK channels.

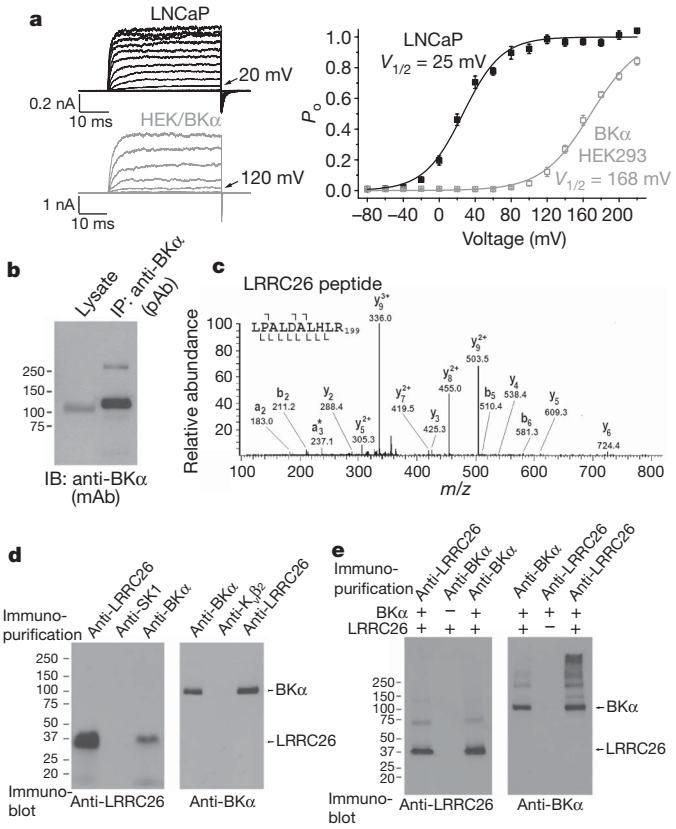

Figure 1 | Identification of LRRC26 as a BK channel accessory protein in LNCaP cells. **a**, Comparison of K^+ currents and the derived P_o–voltage relations for BK channels at $[Ca^{2+}]_i = 0$ in excised inside-out patches of LNCaP cells ($V_{1/2} = 25 \pm 3$ mV, $z = 1.33e \pm 0.10e$, $n = 7$) and BKα-transfected HEK293 cells ($V_{1/2} = 168 \pm 2$ mV, $z = 0.96e \pm 0.06e$, $n = 5$). K^+ currents were recorded in response to depolarization of membrane potential from −80 mV in 20-mV steps. Error bars, s.e.m. **b**, Immunoblot (mouse monoclonal anti-BKα) of BK channels in LNCaP cell lysate and in immunopurified (rabbit polyclonal anti-BKα) channel complex. **c**, MS/MS spectra of a unique peptide of LRRC26 co-immunopurified with LNCaP BK channels. a, b and y indicate different types of peptide fragment in the spectrum. **d**, **e**, Co-immunopurification of LRRC26 and BKα from intact LNCaP cells (**d**) and transiently transfected HEK293 cells (**e**). Proteins were immunopurified with the antibodies indicated at the top and probed with the antibodies indicated at the bottom.

[1]Section of Neurobiology, Center for Learning and Memory, University of Texas, Austin, Texas 78712, USA.

Although association with β-subunits can shift the voltage dependence of activation[3–5], this unprecedentedly large negative shift (~−140 mV) cannot be readily explained by any known modification of the BK channel complex.

The presence of BK channels in LNCaP cells was biochemically confirmed by immunoblot and immunopurification with two antibodies that recognize different regions of the BKα carboxy-terminal domain (Fig. 1b). Analysis of mRNA by PCR with reverse transcription indicated that the BKα in LNCaP cells mainly exists in a normal zero-splicing form (NCBI accession NP_002238). We proposed that an unknown accessory subunit may underlie the observed modification of BK channels in LNCaP cells.

To identify this postulated auxiliary protein, we immunopurified BK channel complexes from LNCaP cells with anti-BKα antibodies (Fig. 1b) and subjected them to liquid chromatography/tandem mass spectrometric (LC–MS/MS) analysis after trypsinization. A ~35-kDa LRR-containing protein, LRRC26 (NCBI accession ABC79623)[13], was identified by LC–MS/MS in immunopurified BK channel complex samples (Fig. 1c), but not in the negative-control samples immunopurified by an antibody against small-conductance calcium-activated potassium channel 1 (SK1). Immunopurification and immunoblot analyses of native LNCaP BK channels (Fig. 1d) show that the anti-BKα antibody can pull down LRRC26 and that the anti-LRRC26 antibody can pull down BKα. Similar specific reciprocal pull-down was obtained when BKα and LRRC26 were co-expressed in heterologous HEK293 cells (Fig. 1e), indicating that LRRC26 is an auxiliary protein of BK channels that can associate with BKα.

We next used microRNA-155-based RNA interference to knock down LRRC26 expression in LNCaP cells. As shown in Fig. 2a, b, the majority (85%) of LRRC26 knockdown cells fully lost the low-$V_{1/2}$ BK channels and instead contained a high-$V_{1/2}$ type of BK channel ($V_{1/2} = 158 \pm 4$ mV at $[Ca^{2+}]_i = 0$), similar to BKα expressed alone. In contrast, most (90%) of the knockdown negative-control cells still fully (40% of cells) or partially (50% of cells) retained the low-$V_{1/2}$ type of BK channel. This suggests that LRRC26 is required for the formation of low-$V_{1/2}$ BK channels in LNCaP cells and that its loss results in a conversion of the BK channels from the low-$V_{1/2}$ type to a typical high-$V_{1/2}$ type. In comparison with the untreated (intact) LNCaP cells, a partial conversion of the BK channels from the low-$V_{1/2}$ type to the high-$V_{1/2}$ type was also observed in 50% of negative-control cells (Fig. 2a). This could be explained by nonspecific suppression of target protein expression by overexpression of control miRNA or green fluorescent protein.

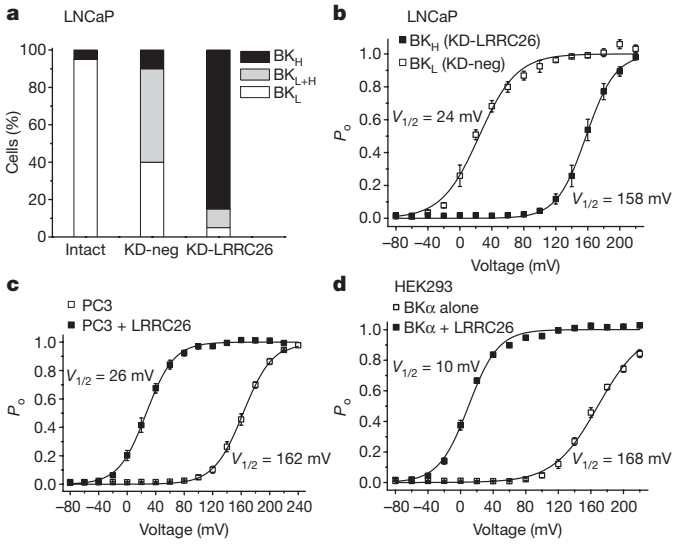

Figure 2 | Co-expression of LRRC26 with BKα is necessary and sufficient for formation of the LNCaP-type low-$V_{1/2}$ BK channels. **a**, Conversion of the low-$V_{1/2}$ BK channels (BK_L) to a typical high-$V_{1/2}$ type (BK_H) after knockdown of LRRC26 expression (KD-LRRC26) in LNCaP cells. BK_{L+H} indicates cells that had both BK_L and BK_H channels. Cells expressing the negative-control miRNA (KD-neg) and untransfected cells (Intact) were used as controls. In total, 20 cells were tested for each group by inside-out patch-clamping at $[Ca^{2+}]_i = 0$. **b**, P_o–voltage relations for the BK_L ($V_{1/2} = 24 \pm 4$ mV, $z = 1.11e \pm 0.03e$, $n = 3$) and BK_H ($V_{1/2} = 158 \pm 5$ mV, $z = 1.55e \pm 0.16e$, $n = 5$) channels at $[Ca^{2+}]_i = 0$ in LNCaP LRRC26 knockdown and negative-control cells. **c**, P_o–voltage relations for BK channels in intact ($V_{1/2} = 162 \pm 3$ mV, $z = 1.31e \pm 0.08e$, $n = 8$) and LRRC26-transfected PC3 cells ($V_{1/2} = 26 \pm 3$ mV, $z = 1.47e \pm 0.11e$, $n = 12$) at $[Ca^{2+}]_i = 0$. **d**, P_o–voltage relations for BK channels formed by BKα alone ($V_{1/2} = 168 \pm 2$ mV, $z = 0.96e \pm 0.06e$, $n = 5$) and together with LRRC26 ($V_{1/2} = 9.7 \pm 1.6$ mV, $z = 1.43e \pm 0.11e$, $n = 5$) in HEK293 cells at $[Ca^{2+}]_i = 0$. Error bars, s.e.m.

LRRC26 is predicted to be a type I single-span membrane protein with a classical amino-terminal cleavable signal peptide for extracellular localization of its large N-terminal LRR domain, which is followed by a single transmembrane domain and a short intracellular C terminus (Fig. 3). The LRR domain consists of five 24-residue LRR motifs with a consensus sequence LXXLXLXXN (where X can be any amino acid) and two cysteine-rich regions called LRRNT and LRRCT flanking its N- and C-terminal sides, respectively (Fig. 3a). LRR domains of various lengths are present in hundreds of proteins, forming a horseshoe-shaped structure with a short α-helix connected by loops flanking the outer circumference and a curved parallel β-sheet lining the inner circumference (Fig. 3b). This β-sheet often provides a versatile structural framework for binding to proteins or other molecules[14,15]. LRRC26 was initially identified as a potential cancer marker protein as it is highly expressed in prostate, breast, colon and pancreas cancer tissues or cell lines[13]. K^+ channels have been demonstrated to govern cell growth of many cancer cells[16], and an upregulated expression of BK channels has also been correlated positively with prostate, bone, and glioma tumours[17–19]. In normal human tissues, LRRC26 mRNA has been found to be most abundant in prostate and salivary glands, and a lower level of expression was detected in the colon, small intestine, stomach, testis and fetal brain[13].

Consistent with the predicted membrane topology, LRRC26 is fully functional in BK channel modulation when its coding sequence is fused to the cytosolic C terminus of the BKα sequence (Supplementary Fig. 3). Functional analyses of LRRC26 deletion mutants indicate that most regions are required for modulatory function of LRRC26 whereas only the putative transmembrane segment is necessary for association to BK channels (Supplementary Fig. 4). LRRC26 is unrelated to the four known BK β-subunits in protein sequence and structure, and thus represents a new type of BK auxiliary subunit. Co-expression of the β1-subunit with the BKα–LRRC26 fusion construct displayed a P_o–voltage relationship and ionic-current kinetics similar to that of BKα–β1 complex alone (Supplementary Fig. 5), suggesting that the β1-subunit can functionally compete with LRRC26.

LRRC26 can modulate BK channels by causing a negative shift of ~−135 to −160 mV in the voltage dependence of BK channel activation, which is equivalent to an apparent effect of $[Ca^{2+}]_i \geq 10$ μM or a free-energy change ($\Delta zFV_{1/2}$) of ~−4 kcal mol^{-1}. However, in spite of the drastically modified voltage dependence, the LRRC26-associated

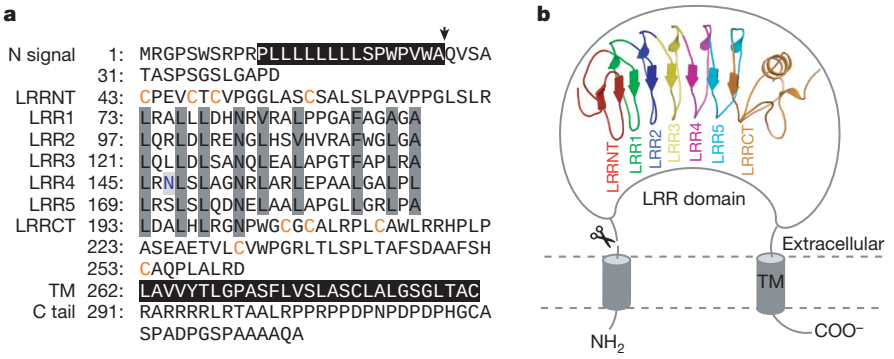

Figure 3 | Properties of LRRC26 protein. **a**, Amino-acid sequence shown in different domains or regions, with conserved residues across LRR units shaded in grey and hydrophobic segments in black. The predicted cleavage site is indicated with an arrow. Cys residues in LRRNT and LRRCT are coloured in orange and the predicted glycosylation site of Asn in blue. TM, transmembrane. **b**, Predicted membrane topology of LRRC26 and modelled structure of the LRR domain based on the X-ray structure (Protein Data Bank ID 2O6S) of the homologous LRR domain of the hagfish variable lymphocyte receptor B59[28].

BK channels still retain a largely unchanged calcium sensitivity (Supplementary Figs 2c–e and 6a), and removal of the Ca^{2+} activation sites[20] has no significant influence on the modulation of BK channels by LRRC26 (Supplementary Fig. 6b).

We investigated the underlying mechanism of LRRC26 modulation in the context of a well-established voltage-dependent allosteric gating model[21]. In the absence of calcium, the relationship between P_o and voltage is determined by two equilibrium constants, namely L, for the closed-to-open (C–O) transition of the pore gate, and J, for the resting-to-activated (R–A) state transition of each individual voltage sensor, and by the allosteric coupling factor, D, between these two events, as follows (Fig. 4a):

$$P_o = \left(1 + \frac{(1+J)^4}{L(1+DJ)^4}\right)^{-1}$$

$$L = L_0 \exp\left(\frac{z_L V}{k_B T}\right)$$

$$J = J_0 \exp\left(\frac{z_J V}{k_B T}\right) \quad (1)$$

The LRRC26-induced large negative shift in $V_{1/2}$ is consistent with its great effect on the kinetics of the ionic K^+ currents (τI_K), which are ~8–20 times slower for deactivation and 3–7 times faster for activation than the high-$V_{1/2}$ channels formed by BKα alone in HEK293 cells (Fig. 4b). The absence of a change in the voltage dependence of τI_K (z_n) at extreme negative voltages (Fig. 4b) indicates that the voltage dependence of C–O (z_L) remains unchanged[21,22]. The P_o–voltage relation of BKα channels alone over a wide voltage range can be fitted with a small variation of previously established BK channel gating parameters[21] (Fig. 4c, d). The LRRC26-induced large negative shift in the P_o–voltage relation might be explained by either a four-order-of-magnitude increase in L_0 (L at zero voltage) or a ~20-fold increase in D, but certainly not by a simple change of the voltage-sensor parameter J_0 or z_J (equation (1) and Fig. 4a), which would profoundly modify the shape of the P_o–voltage curve (Fig. 4c) as previously reported for BK channel voltage-sensor mutants[22]. An increase in L_0 is known to be accompanied by a proportionally elevated P_o value at very negative voltages where the voltage sensors are forced into resting states[21]. The BKα–LRRC26 channel complex still retains a low P_o value similar to that of BKα alone at a very negative voltage, for example −180 mV (Fig. 4d); thus, L_0 is largely not changed. Instead, an increased D value can account well for the P_o–voltage relation at very negative voltages (Fig. 4d). Therefore, we infer that LRRC26 modulates BK channels mainly through a great enhancement (~20-fold) of the allosteric coupling (D) between the voltage-sensor activation and channel opening, which stabilizes both the channel's open state when a voltage sensor is activated and the voltage-sensor activation when the channel is open. The action of LRRC26 seems to be different from that of the BK channel β-subunits, which have complex effects on both voltage and Ca^{2+} sensitivities[23,24]. The modulatory mechanism of LRRC26 is distinct from the action of Ca^{2+}, which

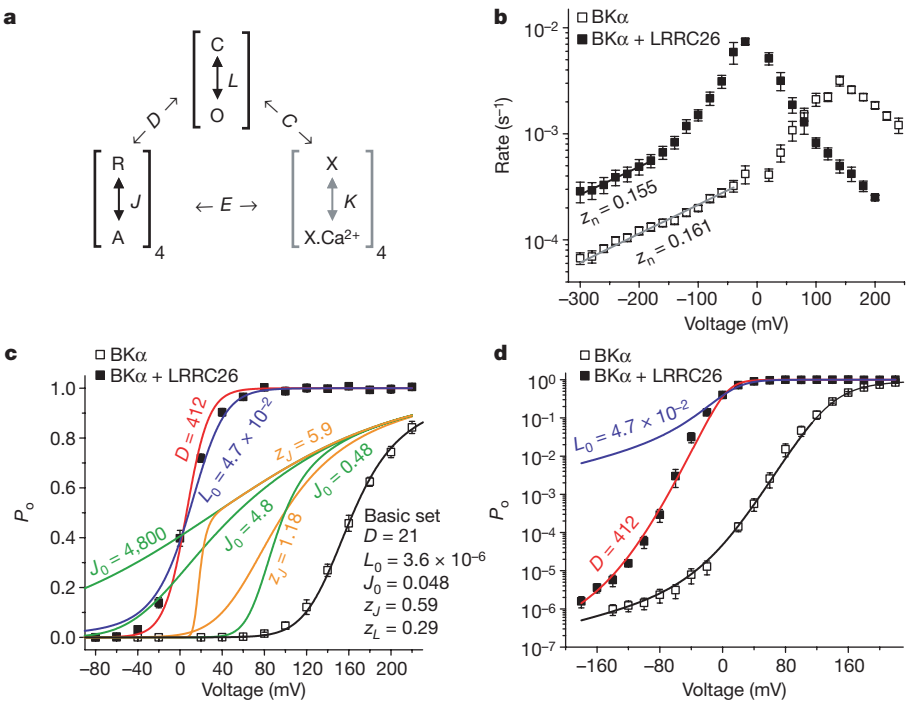

Figure 4 | The LRRC26 modulatory mechanism in the context of the BK channel voltage-dependent allosteric gating model. **a**, Schematic of the allosteric gating model. The three processes of voltage-sensor activation (equilibrium constant J), calcium binding (equilibrium constant K) and channel opening (equilibrium constant L) are related by the three allosteric coupling factors C, D and E. **b**, Kinetics of the BK channel ionic K^+ current (τI_K^{-1}) in the absence and presence of LRRC26 expression. **c**, **d**, Fitting and simulation of the P_o–voltage relations by variation of individual gating parameters over a voltage range for macroscopic currents (**c**) and at very negative voltages, for microscopic currents (**d**). Error bars, s.e.m.

mainly increases L_0 (ref. 21), but is in principle similar to the effect of Mg^{2+}, which also mainly modifies the *D* factor[25], although to a lesser extent. However, we found that LRRC26 modulation does not involve the same pathway as Mg^{2+} in affecting the *D* factor[26] (Supplementary Fig. 7).

In conclusion, we have identified LRRC26 as a novel auxiliary subunit that confers on BK channels an unusual capacity for activation at physiological resting conditions in the absence of elevated $[Ca^{2+}]_i$, thus providing a molecular basis for the activation of BK channels in non-excitable cells (Supplementary Fig. 1b). Even low levels of BK channel activation in non-excitable cells could have a great impact on cellular function because of their large single-channel conductance, which is ~10–20 times larger than that of most other K^+ channels. Because BKα is expressed in a broad spectrum of cells, it is anticipated that this BKα–LRRC26 channel complex might also be present in many other cell types. A low-$V_{1/2}$ BK channel with a similar shift in voltage dependence as that in LNCaP cells was also observed in human T47D breast cancer cells[12] and in mouse and rat inner hair cells[27].

METHODS SUMMARY

Molecular biology and cell culture. Recombinant cDNA constructs of zero-splicing-form human BKα (NCBI accession NP_002238) and C-terminal Myc-tagged LRRC26[13] were used for heterologous expression. HEK293, LNCaP and PC3 cells were obtained from ATCC. To knock down LRRC26 expression in LNCaP cells, nucleotides 326–346 of the human LRRC26 gene (NCBI accession DQ355157) with the flanking sequence of miRNA-155 was constructed into the pcDNA6.2-GW/EmGFP-miR vector (Invitrogen). The commercial pcDNA 6.2-GW/EmGFP-miR-neg control plasmid was employed as negative control of knockdown.

Electrophysiology. K^+ currents were recorded in an inside-out patch configuration with an external solution of 140 mM $KMeSO_3$, 20 mM HEPES (pH 7.20), 2 mM KCl and 2 mM $MgCl_2$. The internal solution contained 136 mM $KMeSO_3$, 20 mM HEPES (pH 7.20) and 6 mM KCl supplemented with 5 mM HEDTA for the $[Ca^{2+}]_i$-free condition or with a certain amount of $CaCl_2$ or $MgCl_2$ buffered by 5 mM HEDTA, nitrilotriacetic acid or EGTA to give the indicated concentration of $[Ca^{2+}]_i$ or $[Mg^{2+}]_i$. The channel open probability (P_o) was calculated from the tail currents by standard procedures. Relationships between P_o and voltage were fitted with a single Boltzmann function, $P_o = (1 + e^{-zF(V - V_{1/2})/RT})^{-1}$, to provide estimates of $V_{1/2}$, the voltage of half-maximal activation, and *z*, the equivalent gating charge.

Immunoblot, immunopurification and mass spectrometry. For immunoblots, BKα and LRRC26 proteins were probed by a mouse monoclonal anti-BKα antibody (L6/60, NeuroMab), recognizing the C-terminal domain of BKα around the S9 region, and a mouse monoclonal anti-LRRC26 antibody raised against the peptide, ARRRRLRTAALRPP, of the LRRC26 C-terminal tail region (X. Liu and I. Pastan, unpublished observations). Immunopurification of BK channels was performed with immobilized rabbit polyclonal anti-BKα antibody, which recognizes the BKα tail region (residues 1,84–1,200) (Alomone Labs), or immobilized mouse anti-LRRC26 antibody. Immunopurification, in-gel digestion, mass spectrometric analysis and the database search were performed as previously described[10].

Full Methods and any associated references are available in the online version of the paper at www.nature.com/nature.

Received 1 February; accepted 7 May 2010.
Published online 7 July 2010.

1. Kolb, H. A. Potassium channels in excitable and non-excitable cells. *Rev. Physiol. Biochem. Pharmacol.* **115,** 51–91 (1990).
2. Salkoff, L., Butler, A., Ferreira, G., Santi, C. & Wei, A. High-conductance potassium channels of the SLO family. *Nature Rev. Neurosci.* **7,** 921–931 (2006).
3. Uebele, V. N. *et al.* Cloning and functional expression of two families of beta-subunits of the large conductance calcium-activated K^+ channel. *J. Biol. Chem.* **275,** 23211–23218 (2000).
4. Brenner, R., Jegla, T. J., Wickenden, A., Liu, Y. & Aldrich, R. W. Cloning and functional characterization of novel large conductance calcium-activated potassium channel beta subunits, hKCNMB3 and hKCNMB4. *J. Biol. Chem.* **275,** 6453–6461 (2000).
5. Behrens, R. *et al.* hKCNMB3 and hKCNMB4, cloning and characterization of two members of the large-conductance calcium-activated potassium channel beta subunit family. *FEBS Lett.* **474,** 99–106 (2000).
6. Barrett, J. N., Magleby, K. L. & Pallotta, B. S. Properties of single calcium-activated potassium channels in cultured rat muscle. *J. Physiol. (Lond.)* **331,** 211–230 (1982).
7. Berkefeld, H. *et al.* BK_{Ca}-Cav channel complexes mediate rapid and localized Ca^{2+}-activated K^+ signaling. *Science* **314,** 615–620 (2006).
8. Fodor, A. A. & Aldrich, R. W. Convergent evolution of alternative splices at domain boundaries of the BK channel. *Annu. Rev. Physiol.* **71,** 19–36 (2009).
9. Schubert, R. & Nelson, M. T. Protein kinases: tuners of the BK_{Ca} channel in smooth muscle. *Trends Pharmacol. Sci.* **22,** 505–512 (2001).
10. Yan, J. *et al.* Profiling the phospho-status of the BK_{Ca} channel alpha subunit in rat brain reveals unexpected patterns and complexity. *Mol. Cell. Proteomics* **7,** 2188–2198 (2008).
11. Tang, X. D., Garcia, M. L., Heinemann, S. H. & Hoshi, T. Reactive oxygen species impair Slo1 BK channel function by altering cysteine-mediated calcium sensing. *Nature Struct. Mol. Biol.* **11,** 171–178 (2004).
12. Gessner, G. *et al.* BK_{Ca} channels activating at resting potential without calcium in LNCaP prostate cancer cells. *J. Membr. Biol.* **208,** 229–240 (2006).
13. Egland, K. A. *et al.* High expression of a cytokeratin-associated protein in many cancers. *Proc. Natl Acad. Sci. USA* **103,** 5929–5934 (2006).
14. Kobe, B. & Kajava, A. V. The leucine-rich repeat as a protein recognition motif. *Curr. Opin. Struct. Biol.* **11,** 725–732 (2001).
15. Bella, J., Hindle, K. L., McEwan, P. A. & Lovell, S. C. The leucine-rich repeat structure. *Cell. Mol. Life Sci.* **65,** 2307–2333 (2008).
16. Kunzelmann, K. Ion channels and cancer. *J. Membr. Biol.* **205,** 159–173 (2005).
17. Cambien, B. *et al.* Silencing of hSlo potassium channels in human osteosarcoma cells promotes tumorigenesis. *Int. J. Cancer* **123,** 365–371 (2008).
18. Bloch, M. *et al.* KCNMA1 gene amplification promotes tumor cell proliferation in human prostate cancer. *Oncogene* **26,** 2525–2534 (2007).
19. Weaver, A. K., Liu, X. & Sontheimer, H. Role for calcium-activated potassium channels (BK) in growth control of human malignant glioma cells. *J. Neurosci. Res.* **78,** 224–234 (2004).
20. Xia, X. M., Zeng, X. & Lingle, C. J. Multiple regulatory sites in large-conductance calcium-activated potassium channels. *Nature* **418,** 880–884 (2002).
21. Horrigan, F. T. & Aldrich, R. W. Coupling between voltage sensor activation, Ca^{2+} binding and channel opening in large conductance (BK) potassium channels. *J. Gen. Physiol.* **120,** 267–305 (2002).
22. Ma, Z., Lou, X. J. & Horrigan, F. T. Role of charged residues in the S1–S4 voltage sensor of BK channels. *J. Gen. Physiol.* **127,** 309–328 (2006).
23. Bao, L. & Cox, D. H. Gating and ionic currents reveal how the BK_{Ca} channel's Ca^{2+} sensitivity is enhanced by its β1 subunit. *J. Gen. Physiol.* **126,** 393–412 (2005).
24. Wang, B., Rothberg, B. S. & Brenner, R. Mechanism of β4 subunit modulation of BK channels. *J. Gen. Physiol.* **127,** 449–465 (2006).
25. Horrigan, F. T. & Ma, Z. Mg^{2+} enhances voltage sensor/gate coupling in BK channels. *J. Gen. Physiol.* **131,** 13–32 (2007).
26. Yang, H. *et al.* Activation of Slo1 BK channels by Mg^{2+} coordinated between the voltage sensor and RCK1 domains. *Nature Struct. Mol. Biol.* **15,** 1152–1159 (2008).
27. Thurm, H., Fakler, B. & Oliver, D. Ca^{2+}-independent activation of BK_{Ca} channels at negative potentials in mammalian inner hair cells. *J. Physiol. (Lond.)* **569,** 137–151 (2005).
28. Kim, H. M. *et al.* Structural diversity of the hagfish variable lymphocyte receptors. *J. Biol. Chem.* **282,** 6726–6732 (2007).

Supplementary Information is linked to the online version of the paper at www.nature.com/nature.

Acknowledgements We are grateful to I. Pastan and X. F. Liu for the generous gift of LRRC26 antibody and plasmids. We thank J. Trimmer for discussion and W. Li, L. Scott, J. Greeson, X. Chen and H. Liu for reading the manuscript. We thank A. Hall, H. Cha and U. Bagaria for research assistance. Mass spectrometry was performed at the UC Davis Proteomics Facility. J.Y. acknowledges postdoctoral fellowship support from the American Heart Association.

Author Contributions J.Y. performed the experiments. J.Y. and R.W.A. designed the research, analysed the data and wrote the paper.

Author Information Reprints and permissions information is available at www.nature.com/reprints. The authors declare no competing financial interests. Readers are welcome to comment on the online version of this article at www.nature.com/nature. Correspondence and requests for materials should be addressed to R.W.A. (raldrich@mail.utexas.edu).

METHODS

Molecular biology and cell culture. Recombinant cDNA constructs of zero-splicing-form human BKα (NCBI accession NP_002238) and C-terminal Myc-tagged LRRC26[13] were used for heterologous expression. For co-expression of BKα and LRRC26 in HEK293 cells, a CMV-promoter-based expression construct containing an internal ribosome entry site between the upstream LRRC26 gene and the downstream BKα gene was made to allow both proteins to be translated from a single bicistronic mRNA with much higher expression of LRRC26 than of BKα. The BKα–LRRC26 fusion construct encodes a fusion protein of human BKα and LRRC26 linked by a short peptide, GKPIPNPRG, between Leu 1103 of BKα and Ser 7 of LRRC26. HEK293, LNCaP and PC3 cells were obtained from ATCC and cultured according to the provider's instructions. Plasmid DNA was transfected into adherent LNCaP or trypsinized PC3 cells with Fugene HD (Roche) transfection reagent, and into HEK293 cells with Lipofectamine 2000 (Invitrogen). The transfected cells were used within 16–57 h post-transfection for electrophysiological analyses. To knock down the LRRC26 expression in LNCaP cells, nucleotides 326–346 of the human LRRC26 gene (NCBI accession DQ355157) with the flanking sequence of miRNA-155 was constructed into the pcDNA6.2-GW/EmGFP-miR vector (Block-iT Pol II miR RNAi Expression Vector Kits, Invitrogen) according to the manufacturer's instructions. The commercial pcDNA 6.2-GW/EmGFP-miR-neg control plasmid expressing a miRNA designed not to target any known vertebrate gene was used as negative control of LRRC26 knockdown. Cells expressing the pre-miRNA were visually selected through co-cistronic expression of EmGFP and electrophysiologically analysed 8 d later after transfection.

Electrophysiology. K^+ currents were recorded in an inside-out patch configuration with an external solution of 140 mM $KMeSO_3$, 20 mM HEPES (pH 7.20), 2 mM KCl and 2 mM $MgCl_2$. The internal solution contained 136 mM $KMeSO_3$, 20 mM HEPES (pH 7.20) and 6 mM KCl supplemented with 5 mM HEDTA for the $[Ca^{2+}]_i$-free condition or with a certain amount of $CaCl_2$ or $MgCl_2$ buffered by 5 mM HEDTA, nitrilotriacetic acid or EGTA to give the indicated concentration of $[Ca^{2+}]_i$ or $[Mg^{2+}]_i$. Experiments were conducted at room temperature (~22 °C). Capacitive transients and leak currents were subtracted by a P/5 protocol at a holding potential of −120 or −150 mV. For macroscopic currents, P_o or G/G_{max} was calculated from the relative amplitude of the tail currents (deactivation, held at −120 or −80 mV). Relationships between P_o and voltage were fitted with single Boltzmann functions, $P_o = (1 + e^{-zF(V-V_{1/2})/RT})^{-1}$, to provide estimates of $V_{1/2}$, the voltage of half-maximal activation, and z, the equivalent gating charge. Single-channel analyses were performed to determine the low P_o values of macroscopic patches at very negative voltages with the program QUB (http://www.qub.buffalo.edu).

Immunoblot, immunopurification and mass spectrometry. BKα and LRRC26 proteins in cell lysates or the immunopurified BK channel complexes were separated by SDS–PAGE (4–20% gradient), transferred to a nitrocellulose membrane and probed by a mouse monoclonal anti-BKα antibody (L6/60, NeuroMab), recognizing the C-terminal domain of BKα around the S9 region, and a mouse monoclonal anti-LRRC26 antibody raised against the peptide, ARRRRLRTAALRPP, of the LRRC26 C-terminal tail domain (X. Liu and I. Pastan, unpublished observations).

Immunopurification of BK channels was performed with protein-A agarose beads covalently crosslinked to the rabbit polyclonal anti-BKα antibody, which recognizes the BKα C-terminal tail region (residues 1184–1200) (Alomone Labs), or with protein-G agarose beads covalently crosslinked to the mouse anti-LRRC26 antibody. BK channel complexes were solubilized from cell membranes with 1% dodecyl maltoside and incubated with immobilized antibodies (1–10 μg) overnight. After repetitive washing (six times), the captured proteins were eluted from affinity beads by Laemmli SDS–PAGE sample buffer (2% SDS, 10% glycerol, 0.001% bromophenol blue, 50 mM DTT and 62.5 mM Tris-HCl (pH 6.8)) and loaded directly to SDS–PAGE gel (4–20% gradient) with a complete run for immunoblot analyses (Fig. 1b) or with a brief run to collect all proteins in one gel band for a single mass spectrometric assay (Fig. 1c).

For mass spectrometric analyses, the BK channel complex and its negative-control sample were immunopurified from LNCaP cells using the anti-BKα and anti-SK1 (anti-$K_{Ca}2.1$, Alomone Labs) antibodies, in-gel digested and analysed using a LTQ-FT hybrid mass spectrometer (Thermo-Fisher) equipped with an UltraPerformance Liquid Chromatography system. In-gel digestion, mass spectrometric analysis and the database search were performed as previously described[10].